

9-9-1991

Determination of the Liquid-Crystal Surface Elastic-Constant K₂₄

David W. Allender

Kent State University - Kent Campus, dallende@kent.edu

G. P. Crawford

Kent State University - Kent Campus

J. W. Doane

Kent State University - Kent Campus

Follow this and additional works at: <https://digitalcommons.kent.edu/physpubs>



Part of the [Physics Commons](#)

Recommended Citation

Allender, David W.; Crawford, G. P.; and Doane, J. W. (1991). Determination of the Liquid-Crystal Surface Elastic-Constant K₂₄. *Physical Review Letters* 67(11), 1442-1445. doi: 10.1103/PhysRevLett.67.1442 Retrieved from <https://digitalcommons.kent.edu/physpubs/12>

This Article is brought to you for free and open access by the Department of Physics at Digital Commons @ Kent State University Libraries. It has been accepted for inclusion in Physics Publications by an authorized administrator of Digital Commons @ Kent State University Libraries. For more information, please contact digitalcommons@kent.edu.

Determination of the Liquid-Crystal Surface Elastic Constant K_{24}

D. W. Allender, G. P. Crawford, and J. W. Doane

Liquid Crystal Institute and Department of Physics, Kent State University, Kent, Ohio 44242-0001
(Received 5 April 1991)

Analysis of the Frank free energy for nematics confined to cylindrical regions indicates that the director pattern is dependent on the surface elastic constant K_{24} if there is weak normal anchoring and escape along the cylinder axis. Using deuterium nuclear-magnetic-resonance techniques on samples of sub-micrometer-size cavities in Nuclepore membranes, we report the first measurement of K_{24} .

PACS numbers: 64.70.Md, 61.30.By, 61.30.Jf, 68.10.Cr

In spite of the fact that the elastic theory of uniaxial nematic liquid crystals has been studied for more than fifty years since the pioneering work of Oseen [1] and Zocher [2], there is still no generally accepted method of determining the so-called surface elastic constant K_{24} . The reason for this has been that K_{24} is irrelevant unless weak anchoring occurs at a surface, and in that case it has proven to be difficult to separate the effects of the anchoring energy from the surface elastic energy. In this paper, analysis and magnetic-resonance measurements are presented which determine both the anchoring

strength and K_{24} by studying director configurations in cylindrically shaped samples with the easy axis for the director normal to the surface. For sufficiently weak anchoring, a new planar-polar director configuration occurs in small-radius samples while at large radii a nonplanar arrangement called the escaped-radial configuration appears [3], as first discussed by Cladis and Kléman [4] and by Meyer [5].

The starting point for the analysis is the elastic free energy, as described by Saupe [6], supplemented by an anchoring energy term [we have used the identity $\hat{\mathbf{n}} \times \text{curl} \hat{\mathbf{n}} = -(\hat{\mathbf{n}} \cdot \text{grad}) \hat{\mathbf{n}}$],

$$F = \int_V d^3r \frac{1}{2} \{K_{11}(\text{div} \hat{\mathbf{n}})^2 + K_{22}(\hat{\mathbf{n}} \cdot \text{curl} \hat{\mathbf{n}})^2 + K_{33}(\hat{\mathbf{n}} \times \text{curl} \hat{\mathbf{n}})^2 - K_{24} \text{div}(\hat{\mathbf{n}} \times \text{curl} \hat{\mathbf{n}} + \hat{\mathbf{n}} \text{div} \hat{\mathbf{n}})\} + \frac{1}{2} \int_S d^2r W_0 \sin^2 \phi. \quad (1)$$

This form for the elastic free energy has been widely used, although the importance of another elastic term (with elastic constant K_{13}) arising due to second derivatives of $\hat{\mathbf{n}}$ has also been studied [7,8] and Schmidt [9] has argued that the terms involving K_{22} and K_{24} should be re-grouped. The validity of neglecting K_{13} is open to question, but is based on having weak deformation and consistently keeping terms only of first derivatives of $\hat{\mathbf{n}}$. If K_{13} is to be included, other terms involving the square of second derivatives of $\hat{\mathbf{n}}$ must also be kept [7,8]. The last term, proportional to the anchoring strength W_0 , is of the Rapini-Papoular form [10], where ϕ is the angle between $\hat{\mathbf{n}}$ and the surface normal. In the strong anchoring limit where $W_0 \rightarrow \infty$, the surface free energy is replaced by the boundary condition $\phi = 0$; i.e., $\hat{\mathbf{n}}$ becomes perpendicular to the surface.

When a liquid crystal is confined to a cylindrical region of radius R and the surface favors ordering in the radial direction, there is competition between the bulk elastic and surface parts of the free energy. Guided by recent experiments [11] and earlier work [4,5], the four configurations shown at the top of Figs. 1 and 2 are studied here. Convenient designations for them are the planar-radial (PR), planar-polar (PP), escaped-radial (ER), and escaped-radial-with-point-defects (ERPD) configurations. Each of the first three director configurations corresponds to a relative minimum in the free energy; the fourth one does not. The ERPD would relax to an ER configuration except that boundary conditions at the ends

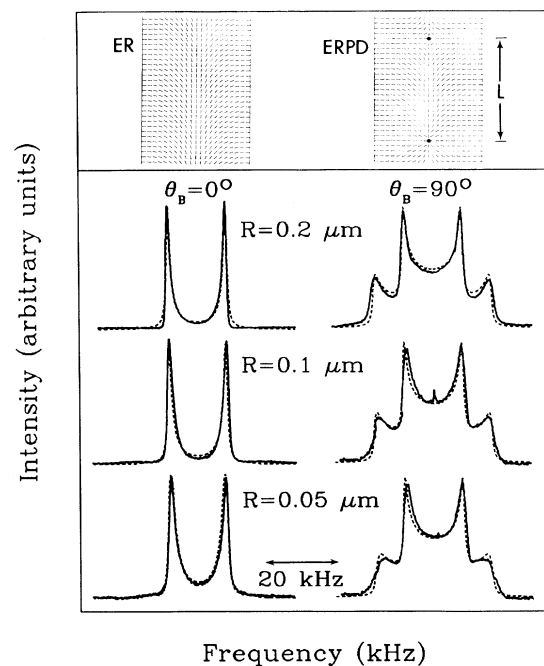


FIG. 1. ^2H -NMR spectra of untreated Nuclepore membranes permeated with $5\text{CB-}\beta d_2$ recorded at $T = 24^\circ\text{C}$. The dashed curve denotes the best fit for σ using the ERPD model. The top panel illustrates the nonplanar nematic director distributions.

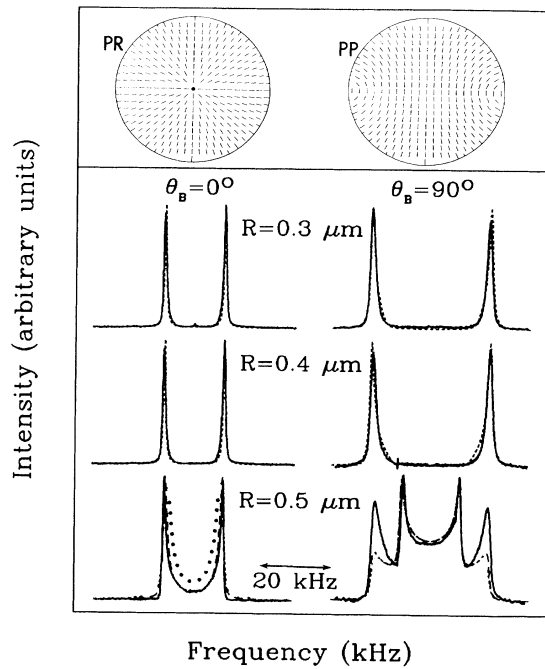


FIG. 2. ^2H -NMR spectra of lecithin-treated Nuclepore membranes permeated with $5\text{CB-}\beta d_2$ recorded at $T=24^\circ\text{C}$. The dashed curve denotes best fit for RW_0/K using the PP model for the $R=0.3$ and $0.4\ \mu\text{m}$ cavities and σ of the ERPD model for the $R=0.5\ \mu\text{m}$ cavity. The dotted curve illustrates the fit for $K_{24}/K=0$. The top panel illustrates the planar nematic director distributions.

of the cylinder are expected to lock in the metastable point defects for the case of real samples. As will be shown in what follows, at large values of the cylinder radii the ERPD configuration is the one which occurs, while at sufficiently small radii it is the planar-polar one unless $K_{11} \ll K_{33}$. It is stressed that the ERPD configuration depends on K_{24} and W_0 separately.

The PR configuration has been considered by others [12,13], so only the results will be given here. In cylindrical coordinates the director is radial and a line singularity exists along the cylinder axis. The singularity may be approximately treated as a cylindrical defect of radius ρ , where ρ is of molecular dimensions. Neither K_{24} nor W_0 contribute to the free energy,

$$F_{\text{PR}} = \pi K_{11} \ln(R/\rho). \quad (2)$$

Although the defect appears to be introduced in an *ad hoc* manner to avoid an infinity in the free energy, it is an approximation to a more accurate description which includes spatial variations not only of \hat{n} but also of the local magnitude of the orientational order [14].

Analysis of the PP configuration is greatly simplified if it is assumed that $K_{11} = K_{33} \equiv K$. While this is not rigorously justifiable, these constants are typically similar except at temperatures slightly above a nematic-to-

smectic transition. The effect of these two constants being different is expected to be small and this could be checked numerically. The director in this configuration is completely specified by $\hat{n} = \cos\Psi\hat{r} + \sin\Psi\hat{\theta}$, where Ψ is the angle between the local director and the radial direction. Note that $\text{div}(\hat{n} \times \text{curl}\hat{n} + \hat{n} \text{div}\hat{n}) = 0$ so that K_{24} is irrelevant for this configuration. The Euler-Lagrange equation for minimizing the elastic free energy then becomes simply the Laplace equation in two dimensions. By symmetry, only the first quadrant of the r - θ plane need be considered.

For the case of strong anchoring $W_0 \rightarrow \infty$, the boundary conditions are $\Psi=0$ at the cylinder surface ($r=R$), $\Psi=0$ for $\theta=\pi/2$, and $\Psi=\pi/2$ for $\theta=0$. The solution is found from conformal mapping to be

$$\Psi(r, \theta) = \pi/2 - \tan^{-1}\{(R^2 + r^2)\tan\theta/(R^2 - r^2)\}.$$

By directly integrating and taking care to exclude a defect region of radius ρ centered at $r=R$, $\theta=0$, the free energy per unit length of the cylinder can now be found to be

$$F_{\text{PP}} = \pi K \ln(R/2\rho). \quad (3)$$

Direct comparison shows the PP configuration to always be of lower free energy than the PR provided that the defects of the two configurations have the same radius ρ and that $K_{11} \approx K_{33} \approx K$.

If weak anchoring occurs at the surface, the boundary condition $\Psi=0$ when $r=R$ is replaced by the relation $\{W_0 \sin\Psi \cos\Psi + K(d\Psi/dr)\}_{r=R} = 0$. The solution of the Euler-Lagrange equation is then

$$\Psi = \pi/2 - \tan^{-1}\{\tan\theta(R^2 + \gamma r^2)/(R^2 - \gamma r^2)\},$$

where $\gamma = [\xi^2 + 1]^{1/2} - \xi$ and $\xi = 2K/W_0R$; the free energy per unit length is

$$F_{\text{PP}} = \pi K \{-\ln(2\xi\gamma) + (1-\gamma)/\xi\}. \quad (4)$$

In the limit $W_0 \gg 2K/R$ (i.e., $\xi \ll 1$),

$$F_{\text{PP}} \approx \pi K \{\ln(W_0R/4K) + 1\} = \pi K \{\ln(eW_0R/4K)\}$$

so that there is a crossover to the strong anchoring limit when $W_0 \sim 2K/\rho e$.

The third possibility, the ER configuration, which has been studied by others [4,5], is now reexamined, taking care to consider the term proportional to K_{24} . The director may be written as $\hat{n} = \cos\Omega\hat{z} + \sin\Omega\hat{r}$, where Ω is the angle between \hat{n} and the cylinder axis. The angle Ω is assumed to depend only on the radial coordinate r . As in the PP case, it is convenient to make the $K_{11} = K_{33} \equiv K$ approximation.

For the case of strong anchoring, the boundary condition is $\Omega(r=R) = \pi/2$, which results in the solution $\Omega = 2 \tan^{-1}(r/R)$ and $F_{\text{ER}} = \pi(3K - K_{24})$. We note that this is the same as reported previously [4,5,13], except for the inclusion of K_{24} .

If weak anchoring occurs, the former boundary condi-

tion is replaced by

$$(d\Omega/dr)|_{r=R} = \sin\Omega \cos\Omega [RW_0 + K_{24} - K]/KR|_{r=R}.$$

Thus, $\Omega = 2 \tan^{-1}[rR^{-1} \tan(\alpha/2)]$, where

$$\alpha = \Omega(r=R) = \cos^{-1}(1/\sigma)$$

and $\sigma \equiv RW_0/K + K_{24}/K - 1$ provided $\sigma > 1$. If $\sigma < 1$, then $\Omega = 0$ everywhere.

The free energy per unit length is

$$F_{ER} = \begin{cases} \pi K \{3 - K_{24}/K - 1/\sigma\} & \text{if } \sigma > 1, \\ \pi K W_0 R / K & \text{if } \sigma < 1. \end{cases} \quad (5a)$$

$$(5b)$$

The ERPD configuration is much more difficult to treat. The angle Ω now depends on both r and the axial coordinate z . Restricting interest to the regime $L/R < 4$ and $\sigma > 1$, a trial solution which has the desired defects and satisfies the boundary condition is of the form $\Omega = \tan^{-1}(\sigma r \{z(1-z/L)(\sigma - [\sigma - 1]r/R)\}^{-1})$ for a cell $r \leq R$, $L \leq z \leq L$. (For $L/R > 4$, a trial form for Ω should closely resemble the pure escaped form.) Periodic repetition of the cell produces a series of defects of spacing L . This trial function gives excellent agreement with numerical solutions of the Euler-Lagrange equation [15]. The resulting free energy per unit length is approximately

$$F_{ERPD} = \pi K \left\{ -\frac{4}{3} \ln \frac{L}{R} + 3 - \frac{K_{24}}{K} + \frac{8}{9} + (3\sigma)^{-1} + (6\sigma^2)^{-1} + \frac{\pi}{5} \left[\frac{\sigma - 1}{\sigma} \right] \frac{L}{R} + \dots \right\}. \quad (6)$$

Although F_{ERPD} is greater than F_{ER} , the point defects of real samples are typically unable to relax by going to the ends of the cylinder. The boundary conditions at the ends effectively repel them, resulting in an array of more or less equally spaced defects. The value of L/R is expected to be sample dependent.

A comparison of the free energies for these four configurations indicates that at large radii the ERPD pattern will occur, but at sufficiently small radii, the PP structure will form. This can be reasoned as follows. As noted above, the PP structure is energetically favored over the PR and the ERPD is metastable with respect to the ER configuration, but unable to relax. Thus, the only remaining question is whether the ERPD or PP structure is favored. Using $R = K/W_0$ as a suitably small R , Eq. (4) gives $F_{PP} = 0.44\pi K$, while Eqs. (6) and (5) imply $F_{ERPD} \geq F_{ER} = \pi K(3 - K_{24}/K - K/K_{24})$ if $K_{24}/K > 1$ ($F_{ER} = \pi K$ if $K_{24}/K < 1$). Therefore, it is expected that at such small radii, the PP configuration will occur unless K_{24} is greater than $2K$. On the other hand, at large R , the planar-polar configuration free energy increases like $\pi K \ln(W_0 R / K)$ while F_{ERPD} approaches a constant independent of R . The precise value of R at which there is a crossover in configuration cannot be predicted because of the uncontrollable parameter L/R .

The measurement of K_{24}/K was made from two independent deuterium nuclear-magnetic-resonance ($^2\text{H-NMR}$) experiments on the liquid-crystal compound 4'-pentyl-4-cyanobiphenyl (5CB- βd_2) in the cylindrical cavities of Nuclepore membranes [16]. The $^2\text{H-NMR}$ spectral pattern directly reflects the distribution of directors in the sample via the angular quadrupole frequencies expressed as $\omega_q(\mathbf{r}) = \pm \pi \delta v_B [3 \cos^2 \theta(\mathbf{r}) - 1]/2$, where $\theta(\mathbf{r})$ is the angle between the nematic director and the magnetic field, and δv_B is the quadrupole splitting of the aligned bulk [17]. The $^2\text{H-NMR}$ spectral patterns are recorded for parallel ($\theta_B = 0^\circ$) and perpendicular ($\theta_B = 90^\circ$) orientations of the cylinder axis relative to the direction of the magnetic field for untreated and lecithin-treated (Sigma Chemical Co.) cavities.

Untreated Nuclepore cavities are found to provide anchoring strengths of sufficient magnitude to support the ERPD structure for radii as small as $0.05 \mu\text{m}$ where the detailed shapes of the $^2\text{H-NMR}$ spectra (see Fig. 1) depend on the surface parameter $\sigma = RW_0/K + K_{24}/K - 1$. The best fits yield values of $L/R = 1.5$ and $\sigma = 8 \pm 0.4$, 4 ± 0.2 , and 2 ± 0.2 for radii $R = 0.2$, 0.1 , and $0.05 \mu\text{m}$. Using a value of $K = 5 \times 10^{-12} \text{ J/m}$, the anchoring strength and the surface elastic constant are determined from σ to be $W_0 = (2 \pm 0.7) \times 10^{-4} \text{ J/m}^2$ and $K_{24}/K = 1 \pm 0.6$.

This measured value of K_{24} was nicely confirmed by modifying the cavity walls with lecithin to weaken the anchoring strength such that the PP structure appears for cavity sizes $R \leq 0.4 \mu\text{m}$ (see Fig. 2). This structure depends only on the value of RW_0/K , which is measured at the $\theta_B = 90^\circ$ orientation to be 1.8 ± 0.2 and 2.4 ± 0.2 for cavities of radii 0.3 and $0.4 \mu\text{m}$, respectively. The PP structure reverts to the ERPD structure at $R = 0.5 \mu\text{m}$ where the spectral fit at $\theta_B = 0^\circ$ yields values of $\sigma = 4.1 \pm 0.2$ and $L/R = 1.5$. Using the value of RW_0/K measured in the PP structure yields values of $K_{24}/K = 1.1 \pm 0.9$. Less satisfying is the $\theta_B = 90^\circ$ case, where the magnetic field becomes a nuisance at larger cavity sizes since the magnetic coherence length $\xi_m = (\mu_0 K / \Delta\chi)^{1/2} / B \sim 1.7 \mu\text{m}$ for the field of the NMR magnet. Comparison of the free energies of the PP and ER configurations using the observed value of the transition $R_c = 0.5 \mu\text{m}$ provides a third check, yielding a value of $K_{24}/K \approx 1.7$.

In conclusion, theoretical analysis reveals that a probe which is sensitive to the director configuration can determine RW_0/K for a sample in the PP configuration for samples of small radius and L/R and $\sigma = RW_0/K + K_{24}/K - 1$ for a large-radius sample in the ERPD pattern. By studying samples where RW_0/K is between 0.1 and 10 , K_{24}/K has been determined.

The K_{24} term in the elastic free energy is nonzero only when the director depends on more than one Cartesian coordinate. Thus previous studies on films in which the director is homogeneous in the plane of the sample were

valid in ignoring K_{24} , but samples with curved surfaces (e.g., cylinders or droplets) or samples with inhomogeneous configurations (e.g., stripes) and weak anchoring should be analyzed in terms of a free energy that includes the K_{24} term.

This research was supported in part by the National Science Foundation under Solid State Chemistry Grant No. DMR 88-176647 and Science and Technology Center ALCOM DMR89-20147.

-
- [1] C. W. Oseen, *Trans. Faraday Soc.* **29**, 883 (1933).
 - [2] H. Zocher, *Trans. Faraday Soc.* **29**, 945 (1933).
 - [3] G. P. Crawford, M. Vilfan, I. Vilfan, and J. W. Doane, *Phys. Rev. A* **43**, 835 (1991).
 - [4] P. E. Cladis and M. Kléman, *J. Phys. (Paris)* **33**, 591 (1972).
 - [5] R. B. Meyer, *Philos. Mag.* **27**, 405 (1973).
 - [6] A. Saupe, *J. Chem.* **75**, 5118 (1981).

- [7] J. Nehring and A. Saupe, *J. Chem. Phys.* **54**, 337 (1971); **56**, 5527 (1972).
- [8] G. Barbero and C. Oldano, *Mol. Cryst. Liq. Cryst.* **168**, 1 (1989); **170**, 99 (1989).
- [9] V. Hugo Schmidt, *Phys. Rev. Lett.* **64**, 535 (1990).
- [10] A. Rapini and M. Papoular, *J. Phys. (Paris), Colloq.* **30**, C4-54 (1969).
- [11] G. P. Crawford, D. W. Allender, J. W. Doane, M. Vilfan, and I. Vilfan, *Phys. Rev. A* **44**, 2570 (1991).
- [12] F. C. Frank, *Disc. Faraday Soc.* **25**, 19 (1958).
- [13] P. G. de Gennes, *The Physics of Liquid Crystals* (Oxford Univ. Press, Oxford, 1974), and references therein.
- [14] Ping Sheng, in *Introduction to Liquid Crystals*, edited by E. B. Priestley, P. J. Wojtowicz, and P. Sheng (Plenum, New York, 1975), Chap. 10.
- [15] S. Zümer (private communication).
- [16] Nuclepore Corp., 7035 Commerce Circle, Pleasanton, CA 94566.
- [17] J. W. Doane, in *Magnetic Resonance of Phase Transitions*, edited by F. J. Owens, C. P. Poole, Jr., and H. A. Farach (Academic, New York, 1979), Chap. 4.